



### III. PASSIVE CANCELLATION COILS (PCC)

#### A. Principle of Operation

In order to obtain the most suitable system geometry both from electromagnetic performance and from the design standpoints, various PCC winding configurations were considered. The final optimized PCC geometry with one and a half PCC winding for each half of the SSTF magnet system [2] with a central gap 250 mm is shown in Fig. 1. The PCC is placed between the BC and the MC. The equivalent circuit of MC, BC and PCC is displayed in Fig. 2 (positions of breakers PB 1, 2, and 3 are given in Table I).

The behaviors of the voltages and currents in the circuit shown in Fig. 2 are described by a set of differential equations with the following initial conditions at  $t = 0$ :  $I_1 = 22.38$  kA,  $I_2 = 0$  kA,  $I_3 = 5.64$  kA and  $E_{MC} = \text{constant}$ , where the subscript 1, 2 and 3 denotes the MC, the PCC and the BC, respectively. In the isothermal case, the resistance of the PCC circuit,  $R_2 = 1$  m $\Omega = \text{constant}$ .

The operating scenario is shown in Fig. 3. It includes the following stages:

- i)  $t_1$ : Charging of the MC starts. The BC is previously charged to 1 T central field (5.64 kA).
- ii)  $t_2$ : The MC field is kept constant during approximately 100 ms, while the discharge of the BC starts with slightly larger than 20 T/s initial ramp rate. The current induced in the PCC increases from approx.  $-1$  kA to 3.8 kA in approximately 55 ms.
- iii)  $t_3$ : The time constant of the PCC circuit is increased by increasing the dump resistance from 1 m $\Omega$  to 14 m $\Omega$  and the PCC current starts to decrease.
- iv)  $t_4$ : The recharging of the MC from +8 T to  $-8$  T starts. To reduce the currents in the BC and the PCC, the resistance of the latter is increased up to 35 m $\Omega$ .
- v)  $t_5$ : The MC starts to discharge from  $-8$  T to 0 T. The currents in the BC and the PCC are relatively low (less than  $-0.5$  kA and  $-1$  kA, respectively).

#### B. PCC Conductor

The PCC conductor must have a low resistance to keep the heat generation low. However, the superconducting conductor in the given case is not the best choice for the following reasons: a) The total circuit resistance involved in the operating scenario is rather high, when compared to the resistance of the PCC itself. b) The conductor must operate in the mode of fast increase of the induced currents and any occasional quench will spoil the PCC operation.

Therefore, it is more reliable in this case to rely on the pure normal conductors with large  $RRR$ . The estimations show that the resistance of such normal conductor is comparable to the resistance of all other necessarily normal parts of the circuits (even if taking into account the worst case of an adiabatic heating of the PCC conductor in the process of shielding).

The PCC is wound onto G-10 bobbins and placed into the cryostat containing the BC. The PCC is cooled with pool-boiling of LHe. The space limitation and the thermal requirement result in the copper conductor reinforced with NbTi with dimension of 17 mm  $\times$  6 mm. Some properties of the conductor are: Cu/NbTi

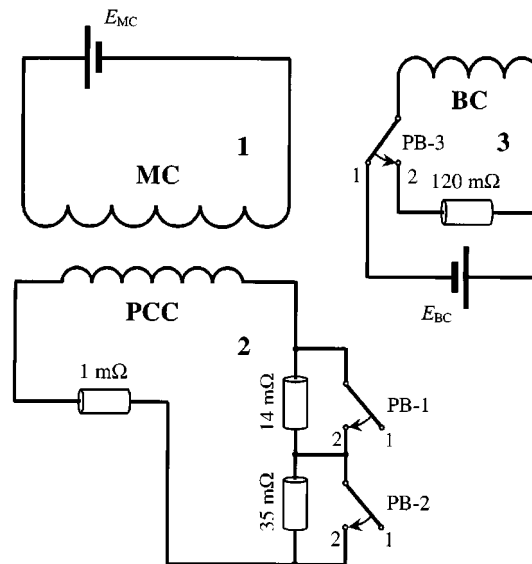


Fig. 2. Electrical circuits of MC, BC, and PCC (PB: power breaker).

TABLE I  
POSITIONS OF BREAKERS

Time range	Position		
	PB-1	PB-2	PB-3
$t_2 - t_1$	1	1	1
$t_3 - t_2$	2	2	2
$t_4 - t_3$	1	2	2
$t_5 - t_4$	1	1	2
$t_6 - t_5$	1	1	2

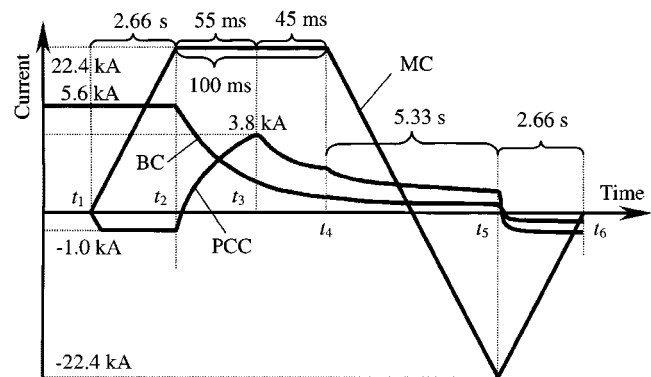


Fig. 3. Operating scenario (not to scale).

ratio is 11 : 1,  $RRR > 200$ , the total volume of copper is about  $1 \times 10^{-2}$  m $^3$ , and the insulation thickness is 1 mm. The NbTi reinforcement practically does not increase the total resistance even when being normal state.

#### C. Results

In Fig. 4, the fields generated by pulsed coils during their discharge processes are shown. It is seen that the field change patterns in the time interval of interest (up to 50 ms) are essentially the same for all cases, BC + CC, BC only, and BC + PCC. It is worth while to note that the field change rate of BC + PCC

can be controlled by varying the BC dump resistance value, to some degree.

In Fig. 5 the BC currents versus time are shown. Note that BCC needs much larger charging current (7 kA) compared to BC only or BC + PCC options. The curve for BC + PCC was calculated for  $R_d = 150 \text{ m}\Omega$  value. It is evident that, by changing  $R_d$  in the interval between 0.1 and 0.15  $\Omega$ , we can get any  $I_{BC}(t)$  curve between the curves for BC only and for BC + PCC shown in Fig. 5. This additional degree of freedom can be helpful during the tests of short samples or TF coils.

In Fig. 6 the inductive increase of the MC current is compared for the cases of BC only and BC + PCC assuming no control from the MC power supply. It is seen that, in the latter case, the current increase is much less and slow, so the requirements to the MC power supply control system are much easier.

The above results were calculated for the isothermal case, when temperature (and, hence, the resistance of the PCC conductor) is constant during BC discharge process. Actually, there is some heating of the PCC conductor mainly due to its Joule heating (according to the calculations, the eddy currents heating is negligible small compared to the Joule heating and may not be taken into account). The worst adiabatic case corresponds to the total absence of heat transfer. This adiabatic case was calculated numerically using the same set of equations, but taking into account the adiabatic heating of the PCC conductor after each step ( $\Delta T = 1 \text{ K}$ ), driven by its heat capacity and resistivity. The results of calculations show that i) the maximum PCC adiabatic temperature during BC discharging process is below 28 K; ii) the currents in the adiabatic case and in isothermal case for the BC are practically coincide, while, for the PCC, they are slightly different (only after  $t_4$ , see Fig. 3).

Fig. 7 illustrates the field change rates in the most presumably dangerous region of the MC during the BC discharge. One can see from the figure that, during the MC standby,  $\dot{B}$  components values practically do not exceed 1 T/s. It is also seen that, even with only two dump resistors in the PCC circuit, the PCC system is flexible and can fit the MC field change to the various complicated scenarios as was analyzed in this paper. The flexibility is due to the possibility to change the values of dump resistances and the moments of their on/off switching.

Other advantage of the BC + PCC concept is that the forces acting between the halves of the system are much less than those of the BC + CC case. For the case of BC + CC, the maximum forces are of order of 1000 kN (repulsive ones in the case of  $B_{BC} = -1 \text{ T}$  and attractive ones in the case of  $B_{BC} = +1 \text{ T}$ ). For the case of BC only, the maximum force is attractive both for  $B_{BC} = \pm 1 \text{ T}$  (approximately 50 kN for  $B_{BC} = -1 \text{ T}$  and 14 kN for  $B_{BC} = +1 \text{ T}$ ). The maximum forces for BC + PCC remain the same. So, the forces are several dozens time smaller than those for BC + CC. It is also important to note that they are essentially attractive. The maximum repulsive force does not exceed 4 kN.

#### IV. CONCLUSION

The PCC geometry has been optimized and a proper conductor has been designed. The analysis regarding extra fields, field ramps and currents induced by the BC-PCC in the MC

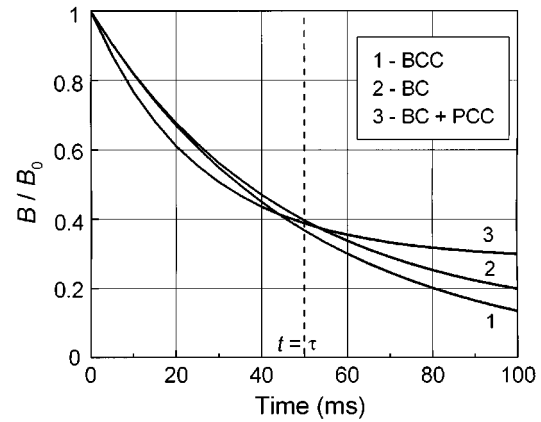


Fig. 4. Pulsed central field (in arbitrary units) versus time.

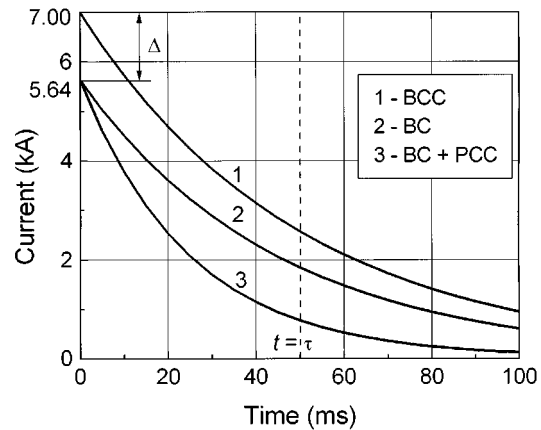


Fig. 5. BC current versus time.

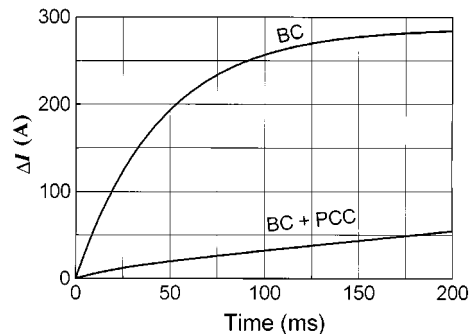


Fig. 6. MC inductive current increase ( $\Delta I = I - I_{op}$ ) for cases BC + PCC and BC only.

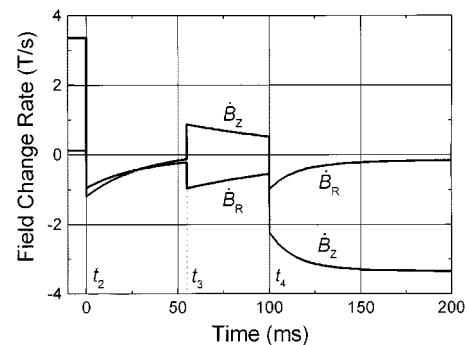


Fig. 7. Field change rate components versus time between  $t_2$  and  $t_4$  (see Fig. 3) in the most dangerous point ( $R = 382 \text{ mm}$ ,  $Z = 285 \text{ mm}$ ) of MC.

has been performed. It is shown that the PCC approach has several important advantages over the BCC approach. It is especially true to the attractive forces between two halves of the PC system. It is shown that the PCC has the merits as follows:

- The PCC reduces  $\dot{B}$  acting on the MC from the BC, about three times better while the active CC even increases it, giving the MC the danger of quench.
- The compactness of the PCC allows the placement in the gap between the MC and the BC, where it acts more effectively.
- The PCC allows the structure to avoid the strong forces acting between the active CC and the BC.
- The PCC allows the BC to operate at considerably lower currents.
- The PCC allows the flexibility in ramp rate and convenience for experiments by changing the resistances in the PCC circuit.

It is shown that the proposed BC + PCC system is preferable to the previously proposed BC + CC system.

#### REFERENCES

- [1] S. Baang, S. H. Baek, H. J. Choi, E. J. Chung, Y. B. Chang, and J. H. Kim *et al.*, "The test facility for the KSTAR superconducting magnets at SAIT," *IEEE Trans. Appl. Superconduct.*, vol. 10, pp. 645–648, Mar. 2000.
- [2] S. Baang, K. Kim, Y. Kim, H. Park, S. Kim, and Q. Wang *et al.*, "The background magnets of the Samsung Superconductor Test Facility (SSTF)," *IEEE Trans. Appl. Superconduct.*, vol. 11, pp. 2082–2085, Mar. 2001.
- [3] Q. L. Wang, S. Baang, C. S. Yoon, S. B. Kim, H. K. Park, and M. K. Kim *et al.*, "Induced voltage and alternating current loss in superconducting magnet system for SSTF," *IEEE Trans. Appl. Superconduct.*, vol. 11, pp. 2074–2077, Mar. 2001.